Supplement of Atmos. Chem. Phys., 23, 13769–13790, 2023
https://doi.org/10.5194/acp-23-13769-2023-supplement
© Author(s) 2023. CC BY 4.0 License.

Atmospheric Chemistry and Physics
Open Access
EGU

Supplement of

Air pollution trapping in the Dresden Basin from gray-zone scale urban modeling

Michael Weger and Bernd Heinold

Correspondence to: Michael Weger (weger@tropos.de)

The copyright of individual parts of the supplement might differ from the article licence.

1 Model validation with ground-based in-situ measurements

For a concise validation of the CAIRDIO simulations, meteorological (wind speed, wind direction, air temperature) and BC observations are inferred from two air-monitoring sites operated by the LfULG. Station Dresden-Winckelmannstr. (labeled DW) is located within the Dresden Basin in the southern part of Dresden, while station Radebeul-Wahnsdorf (labeled RW) is located above the basin on a lift to the northwest of the city (see Fig. 4). Both stations are classified as background stations since the closest major roads are more than $50\,\mathrm{m}$ distant from station DW (average daily traffic count, ADTC of 27430 vehicles), and more than $100\,\mathrm{m}$ from station RW (ADTC of 4330 vehicles). Besides the different larger-scale environments the stations are situated in (urban background within the basin for station DW, rural background above the basin for station RW), the closer building environment is different for the two stations, as depicted by the sky-view simulations in Fig. S7. Station DW is entirely surrounded by buildings, even though the average distance of most buildings from the measurement site is above $50\,\mathrm{m}$. This results in a sky-view factor of 0.84. The most significant obstruction is a roughly $25\,\mathrm{m}$ tall building about $60\,\mathrm{m}$ to the northeast of the site. Significant tree cover is also present mainly to the east, south, and west of the site (not shown). The wind measurements can thus not be regarded to be entirely representative of the prevailing wind conditions within the Dresden Basin. In contrast to site DW, site RW provides a mostly unobstructed view of the sky (sky-view factor of 0.94). The only significant obstacle near the site is a lattice tower ($35\,\mathrm{m}$ height) located $15\,\mathrm{m}$ to the northwest of the station.

The comparisons of modeled wind speed with hourly wind speed measurements for the two simulation periods are shown in Fig. S1a (period T1) and b (period T2). The measured wind speed in the Dresden Basin at site DW (grey lines) is generally low throughout the simulation periods as it fluctuates around $1\,\mathrm{m\,s^{-1}}$. The fluctuations seem to temporarily follow a diurnal cycle with the lowest wind speeds (near calm conditions) generally occurring during the night-time hours. During period T1, the modeled wind speed (red lines) generally follows the measured profile well, as it reproduced the observed fluctuations and magnitude in wind speed. Nevertheless, the model overestimates the wind speed during some calm events during period T2, which suggests that the nocturnal boundary layer is not always accurately represented in the model. Without additional measurements to resolve the vertical structure of the boundary layer, this is, however, impossible to verify. At site RW located outside the Dresden Basin, the measured wind speed (black lines) is consistently higher than at site DW and reaches occasionally up to $5\,\mathrm{m\,s^{-1}}$. Partly, this difference is also a result of the more unobstructed environment station RW is located within. The model (blue lines) again follows this trend well, even though there are also periods when the model significantly overestimates wind speed by at least $2\,\mathrm{m\,s^{-1}}$ (1 March of period T1, 3-4 June of period T2). Concerning the validation of the wind direction, only the comparison for site RW is shown (Fig. S1c-d), as site DW is more influenced by buildings and would demand a higher resolved simulation for a representative comparison. The measured wind direction profiles at site RW express the variable synoptic influence. For example, they show the sequence of northwesterly and southeasterly winds, which the model generally follows quite well, especially during period T1. Significant disagreements occur on 31 May and on 5-6 June, when the model shows a more easterly wind direction instead of westerly to northwesterly winds. These disagreements are also seen in the mesoscale precursor runs with the model COSMO-MUSCAT (not shown). In Fig. S1e and f, measured profiles of the near-surface air temperature are compared with model results. Generally, the differences between the sites DW and RW are only marginal. Most of the time though, site DW shows higher temperatures than site RW, which is a result of the different elevations of the sites ($112\,\mathrm{m}$ vs. $246\,\mathrm{m}$ above sea level). During a few nights, however, the air temperature at site DW dropped below the temperature at site RW, which indicates the presence of a diurnal CAP within the Dresden Basin (e.g. from 3 to 4 March). The model generally follows the measured temperature evolution well, especially in the longer term. For some individual diurnal cycles, however, the model deviates from the measurements by up to $5\,\mathrm{K}$, and this is irrespective of the site. In particular, during some nights (3-4 March, 1-2 June, and 5-6 June) the modeled air temperature did not drop as low as the measurements show. Similar deviations are again seen in the mesoscale precursor simulations (not shown), which is not surprising given that a surface temperature interpolation scheme is used instead of a prognostic surface model. Lastly, Fig. S1g and h show the BC measurements and comparable model results of dispersion experiment BC-full (using realistic emissions plus realistic boundary conditions from the COSMO-MUSCAT simulation D3). During period T1, a clear relationship between a southeasterly to southerly wind direction and elevated BC concentrations at site DW (peaks above $2\,\mathrm{\mu g\,m^{-3}}$) can be observed, which to a lesser extent applies also to site RW. The only notable exception is a marked peak (above $4\,\mathrm{\mu g\,m^{-3}}$) at site DW during the night from 5-6 March, which is not present at site RW. During this time the prevailing wind direction outside the Dresden Basin was from the west, but due to the stable stratification calm wind conditions resulted within the

basin at site DW. For the rest of the time, BC concentrations were mostly below $1\,\mu g\,m^{-3}$. Model results at site DW show a similar pattern, even though the aforementioned prominent peak from 5-6 March is missed by the model, probably as a result of an underestimated stability of the boundary layer during this time. Based on the computed fractional bias (FB) the model significantly underestimates BC concentrations at both sites RW ($FB = 0.75$) and DW ($FB = 0.39$). Since the urban emissions and orographically induced air-pollution trapping effects have a larger influence on BC concentrations at site DW compared to site RW, the better model agreement at site DW suggests that the regional BC background concentrations are significantly underestimated. This is confirmed by the comparison with the mesoscale model run D3, which shows a similar underestimation for site RW (not shown). In this regard, it is noteworthy that simulation period T1 was influenced by the second wave of the COVID-19 pandemic, which may have resulted in reduced traffic emissions in reality. Adjusting our prescribed emissions downward to account for this would likely have resulted in a still larger underestimation of BC concentrations. Compared to period T1, the relationship between the prevailing wind direction and the measured BC concentration is much less clear during period T2, and the average BC concentrations (most of the time below $1\,\mu g\,m^{-3}$) are significantly lower compared to period T1. While the model still underestimates BC concentrations, the difference is this time much smaller ($FB = 0.20$ at site RW and $FB = 0.40$ at site DW) but likely of the same cause as for period T1, i.e. an underestimated regional BC background.

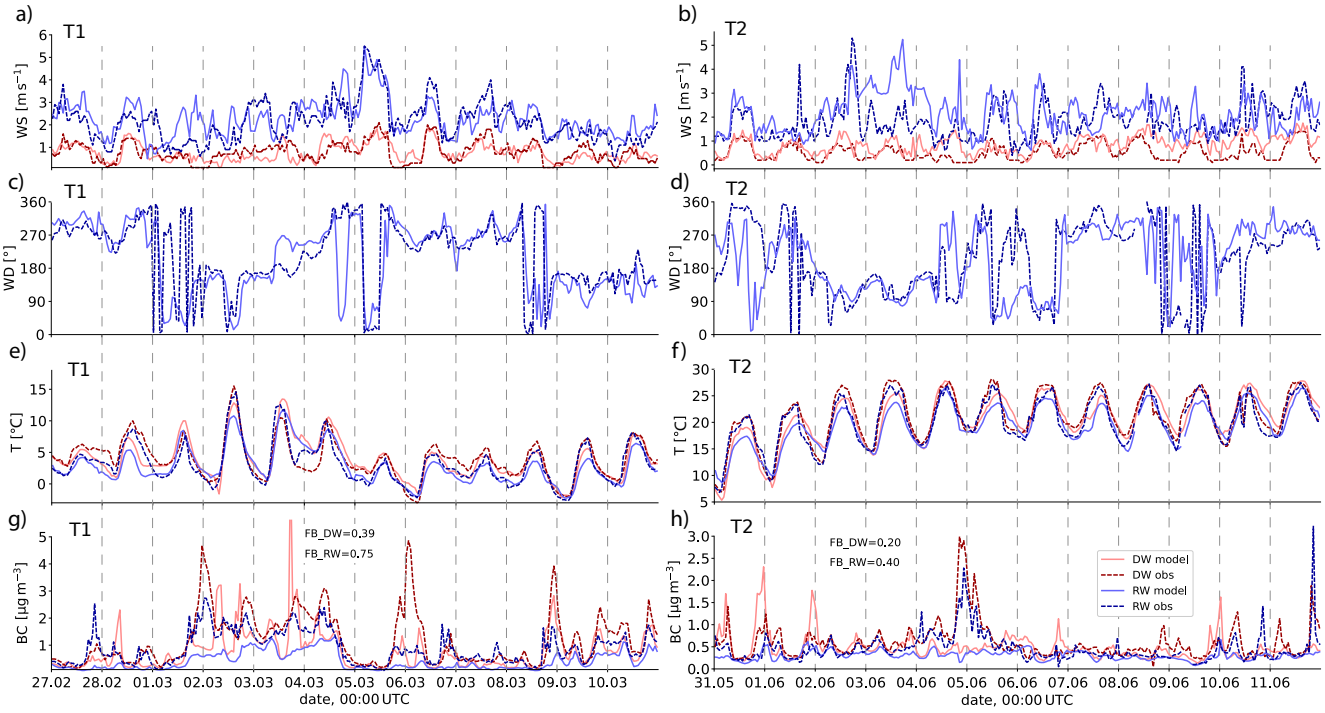

Figure S1. Model evaluation of run BC-full with meteorological and air-quality measurements from two background air-monitoring sites (site DW located within the Dresden Basin, site RW located on a lift to the north of the Dresden Basin, see Fig. 4). (a) and (b) show the comparison for the wind speed, (c) and (d) for wind direction (for site RW only), (e) and (f) for air temperature, and (g) and (h) for the BC concentration. For the BC concentration, the time-average fraction biases (FB) between measurements and model results are computed. Measurements from sites DW and RW are shown by dashed red and blue lines, respectively. Model results at the sites DW and RW are shown by full red and blue lines, respectively.

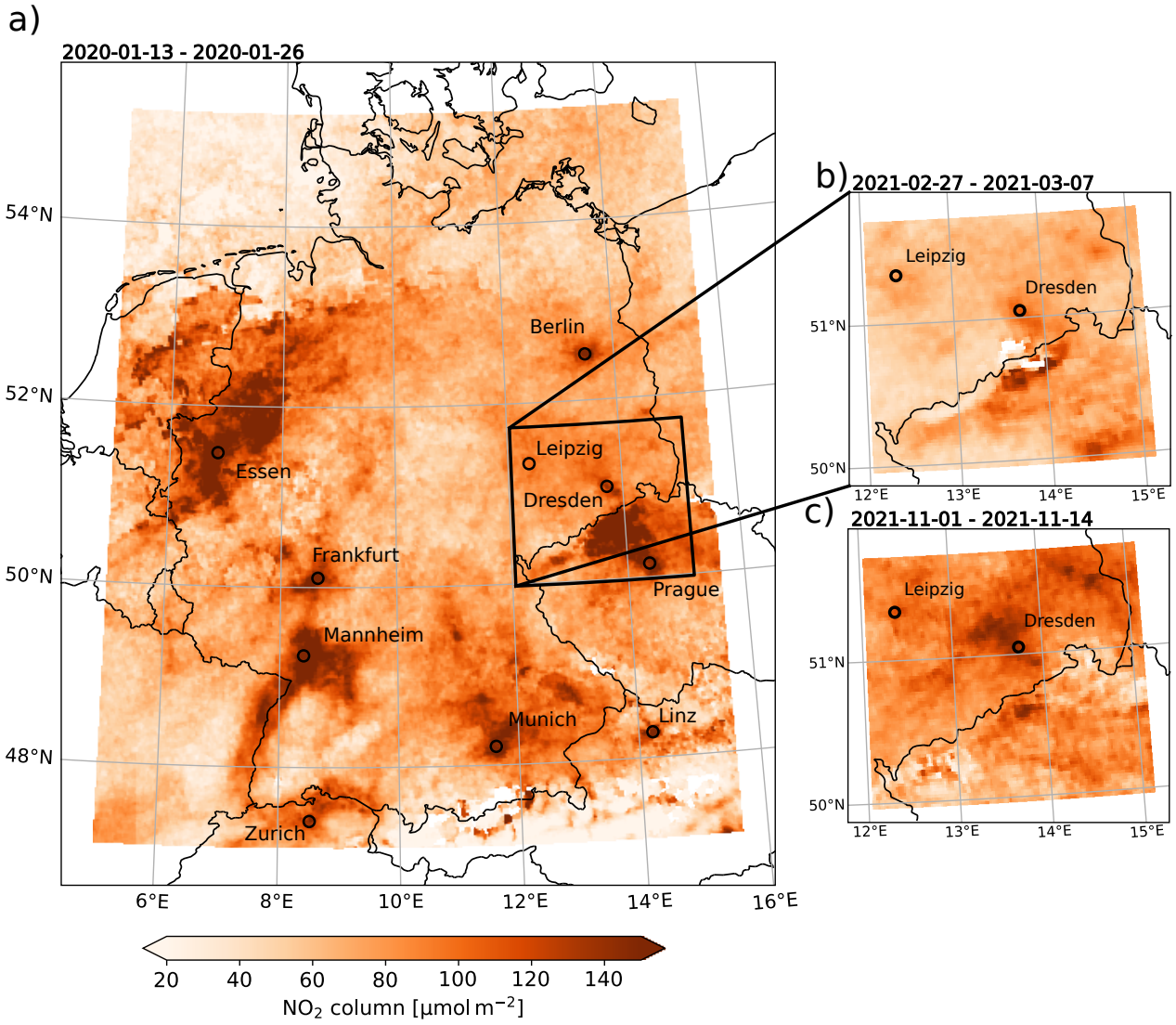

Figure S2. (a) Reprocessed Sentinel-5P satellite NO_2 vertical column product averaged over 14 days showing air pollutant accumulations in the Dresden Basin and in other areas of Germany, Switzerland, Austria, and the Czech Republic during predominantly stable winter weather conditions, which prevailed from mid to late January 2020. (b) and (c) show the same NO_2 product for a smaller area indicated by the black box (a) during two similar periods in 2021, when air pollution accumulated in the Dresden Basin. For comparison, the city of Leipzig is further shown on the maps, which is of similar size as Dresden but has mostly a flat surface orography. The data shown was obtained from the Copernicus Sentinel-5P Mapping Portal.

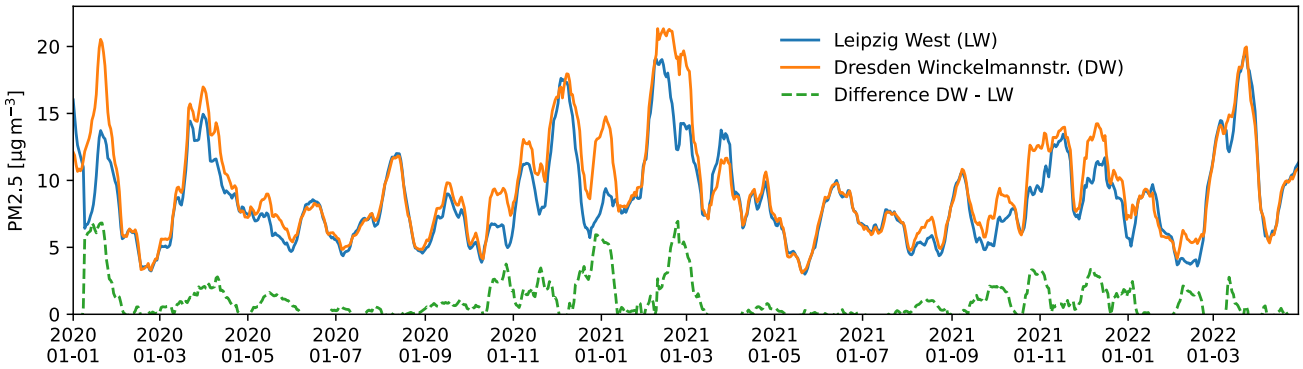

Figure S3. 14-days moving average of urban background PM2.5 concentrations observed at stations of the Saxon air quality monitoring networks in Leipzig (Leipzig West, blue line) and in Dresden (Dresden Winckelmannstr., orange line) from January 2020 to April 2022. The green dashed line shows the difference between Dresden and Leipzig, which is largest during the winter months and suggests air pollution trapping in the Dresden Basin.

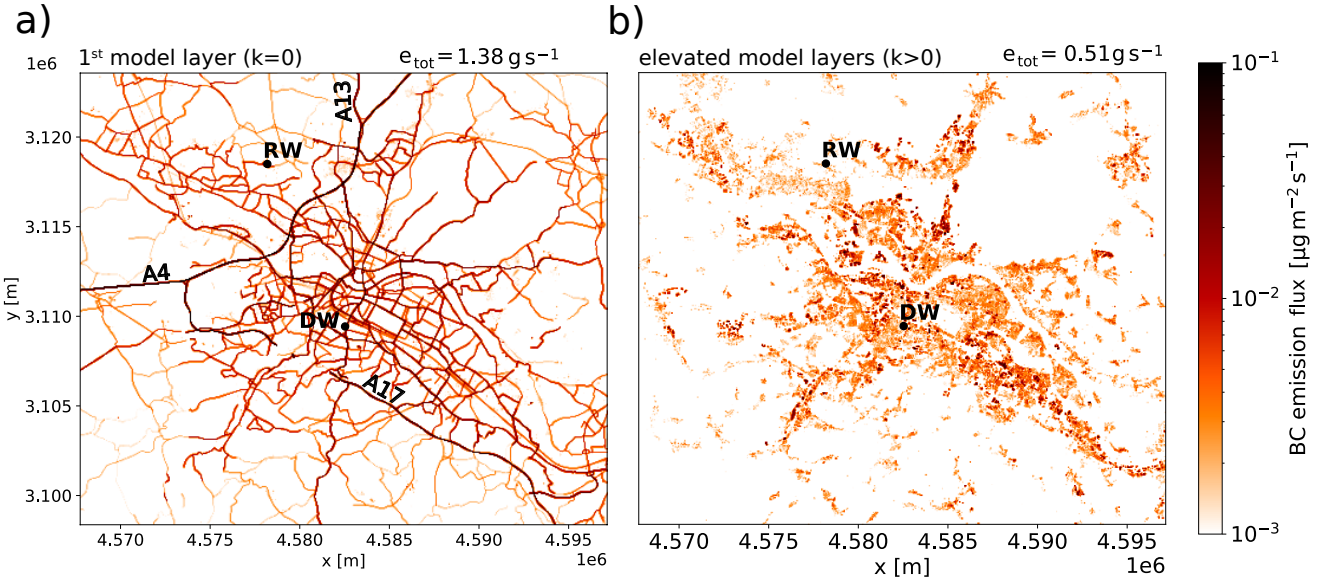

Figure S4. (a) shows the distribution of BC emissions within the first vertical layer of domain D4, (b) shows the vertical sum of BC emissions from industrial sites and residential buildings over all elevated model layers (model layer index $k > 0$). e_{tot} is the total BC emission area sum of the first model layer and of all elevated model layers, respectively. The positions of the background air-monitoring stations DW and RW are indicated by black dots and labels. The highways A4, A13, and A17 are also indicated in (a).

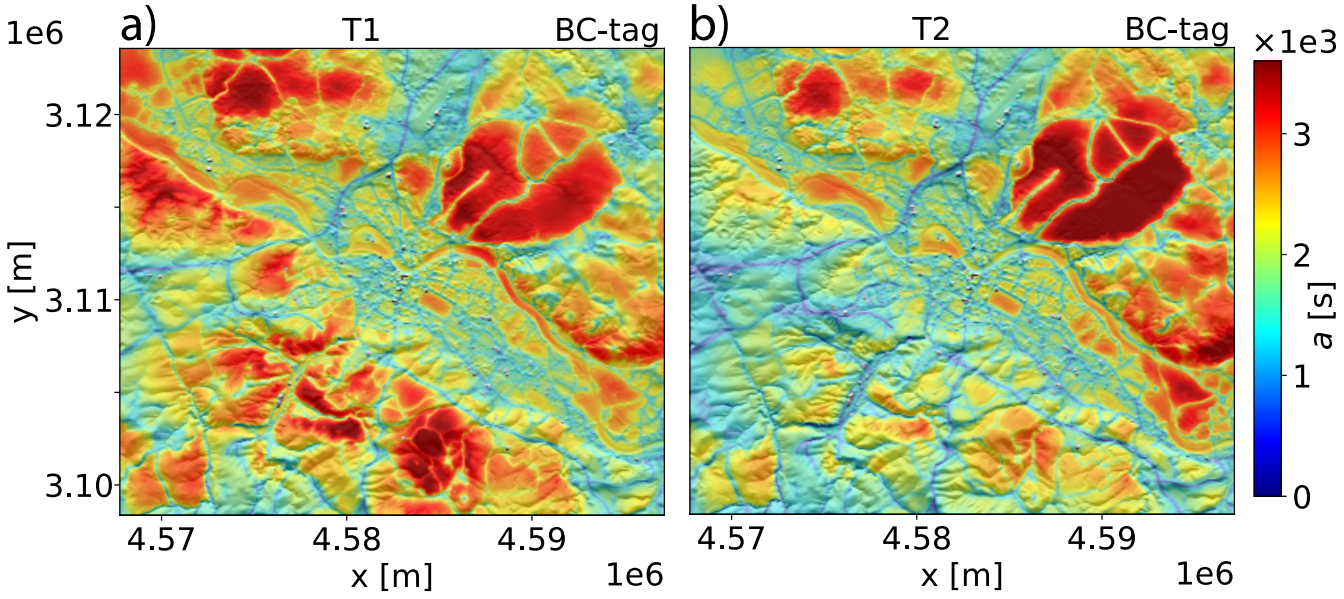

Figure S5. Temporal mean particle age a_{BC} patterns of dispersion experiments BC-tag as computed by CAIRDIO. The pattern (a) refers to the simulation period T1 (27 February - 10 March 2021), the pattern (b) to period T2 (31 May - 11 June 2021).

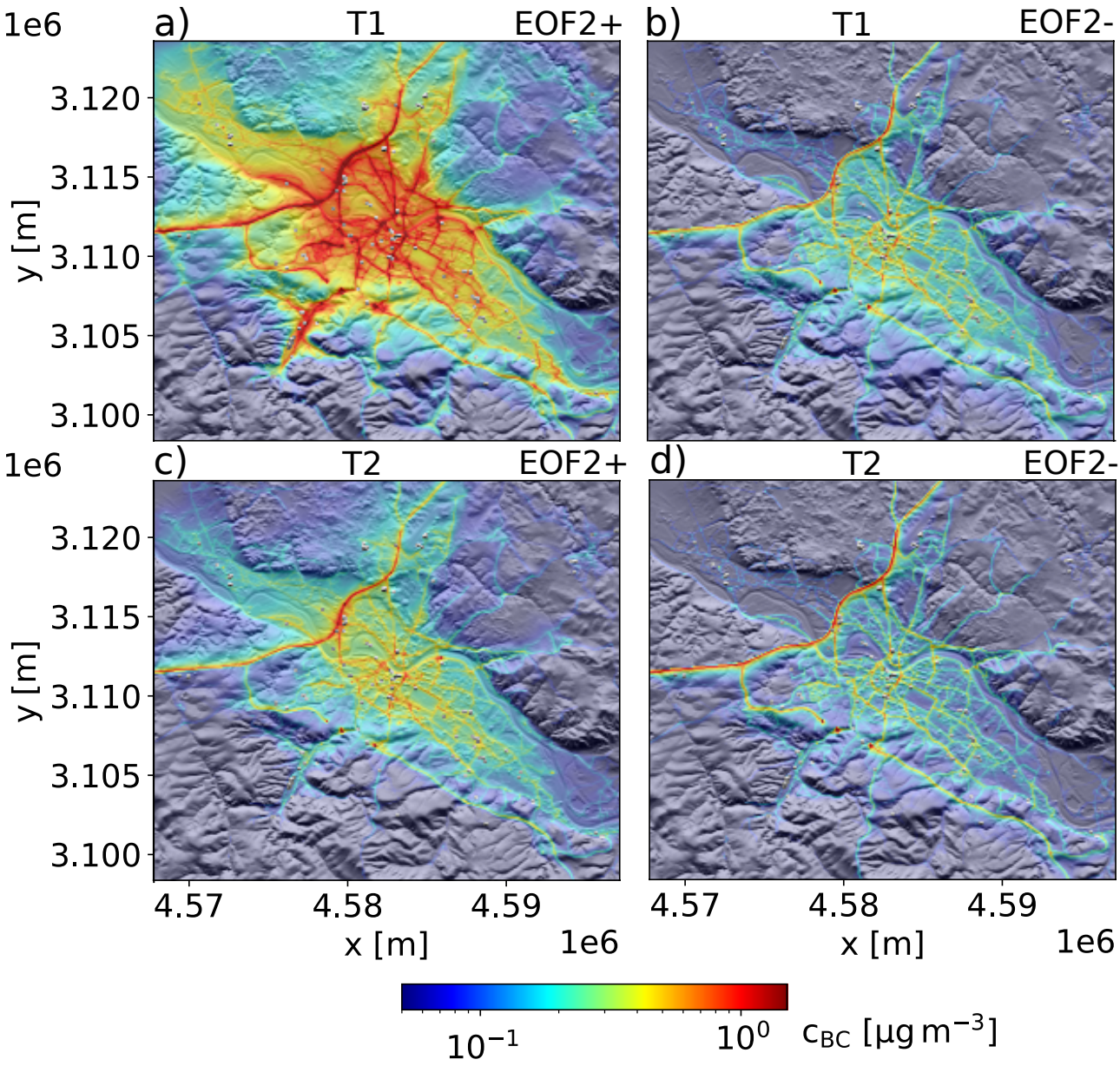

Figure S6. Time-weighted average BC concentration patterns within the first model layer computed for periods of a positive and negative amplitude of the second EOF, respectively. The patterns (a) and (b) refer to the late winter period T1 (27 February - 10 March 2021), and the patterns (c) and (d) to the early summer period T2 (31 May - 11 June 2021).

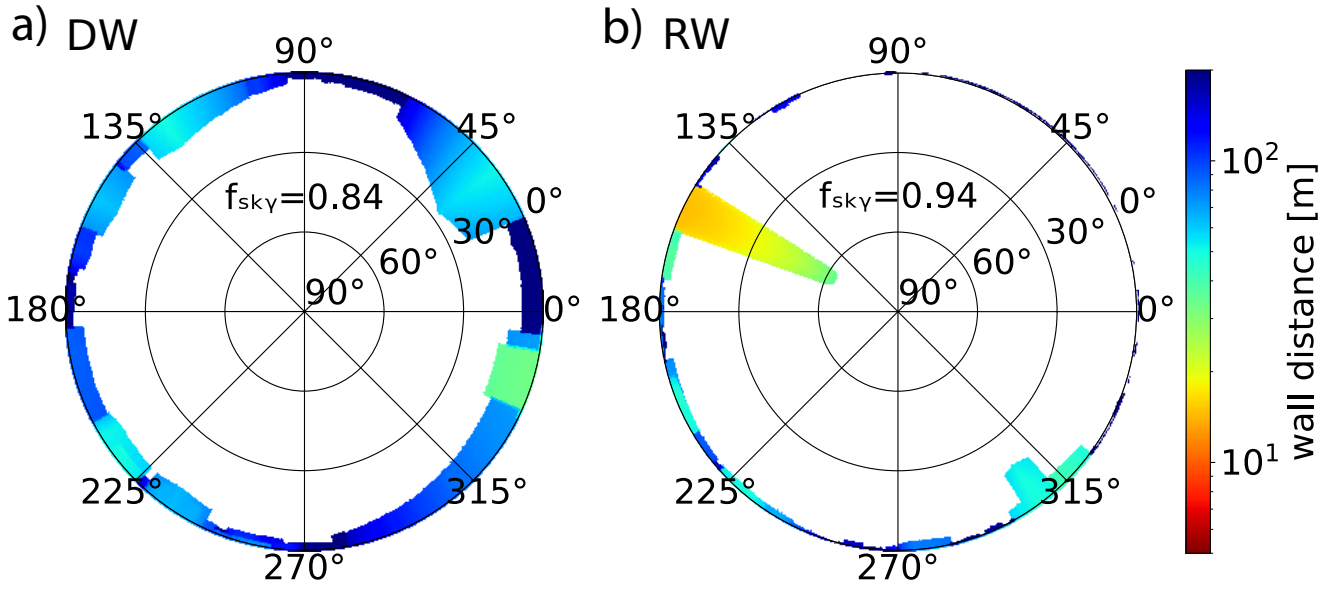

Figure S7. Simulated view on surrounding buildings in spherical coordinates at the exact 3-D locations of the inlets for the Saxon air quality monitoring stations (a) Dresden, Winckelmannstraße (DW), and (b) Dresden, Radebeul Wahnsdorf (RW). The colors indicate the distance of instrument inlets to building walls, while the visible sky is shaded in white. Additionally, the sky-view factors f_{sky} are computed as the fraction of the solid angle of the hemisphere not blocked by buildings.